Published in final edited form as:
Cancer Res. 2013 September 15; 73(18): 5821–5833. doi:10.1158/0008-5472.CAN-13-1080.

ANTXR1, a stem cell enriched functional biomarker, connects collagen signaling to cancer stem-like cells and metastasis in breast cancer

Daohong Chen[1], **Poornima Bhat-Nakshatri**[1], **Chirayu Goswami**[4], **Sunil Badve**[3], and **Harikrishna Nakshatri**[1,2,*]

[1]Department of Surgery, Indiana University School of Medicine, Indianapolis, Indiana, USA 46202

[2]Department of Biochemistry & Molecular Biology, Indiana University School of Medicine, Indianapolis, Indiana, USA 46202

[3]Department of Pathology & Laboratory Medicine, Indiana University School of Medicine, Indianapolis, Indiana, USA 46202

[4]Centre for Computational Biology & Bioinformatics, Indiana University School of Medicine, Indianapolis, Indiana, USA 46202

Abstract

Cancer stem-like cells are thought to contribute to tumor recurrence. The anthrax toxin receptor ANTXR1 has been identified as a functional biomarker of normal stem cells and breast cancer stem-like cells. Primary stem cell-enriched basal cells (CD49f+/EpCAM−/Lin−) expressed higher levels of ANTXR1 compared to mature luminal cells. CD49f+/EpCAM−, CD44+/EpCAM−, CD44+/CD24− or ALDEFLUOR-positive subpopulations of breast cancer cells were enriched for ANTXR1 expression. CD44+/CD24−/ANTXR1+ cells displayed enhanced self-renewal as measured by mammosphere assay compared to CD44+/CD24−/ANTXR1− cells. Activation of ANTXR1 by its natural ligand C5A, a fragment of collagen VI α3, increased stem cell self-renewal in mammosphere assays and Wnt signaling including the expression of the Wnt receptor LRP6, phosphorylation of GSK3α/β and elevated expression of Wnt target genes. RNAi-mediated silencing of ANTXR1 enhanced the expression of luminal-enriched genes but diminished Wnt signaling including reduced LRP6 and ZEB1 expression, self-renewal, invasion, tumorigenicity and metastasis. ANTXR1 silencing also reduced the expression of HSPA1A, which is overexpressed in metastatic breast cancer stem cells. Analysis of public databases revealed ANTXR1 amplification in medullary breast carcinoma and overexpression in estrogen receptor-negative breast cancers with the worst outcome. Further, ANTXR1 is among the 10% most overexpressed genes in breast cancer and is co-expressed with collagen VI. Thus, ANTXR1:C5A interactions bridge a network of collagen cleavage and remodeling in the tumor microenvironment, linking it to a stemness signaling network drives metastatic progression.

Keywords

ANTXR1; breast cancer; cancer stem cells; collagen VI; metastasis

*Corresponding Author: Harikrishna Nakshatri, C218E, 980 West Walnut St, Indianapolis, IN 46202, USA. hnakshat@iupui.edu.
Authors have no conflict of interest to declare.

Introduction

Breast cancer represents a diverse group of tumors with heterogeneous morphology, molecular profiles, therapeutic sensitivity, and outcome (1, 2). A subset of breast tumors suggested to contain a minor population of cancer cells termed cancer stem cells (CSCs). CSCs are believed to contribute to tumor heterogeneity, therapeutic resistance, and metastasis (3). CSCs are typically isolated using cell surface markers such as CD44, CD24, DNER, DLL1, and CD271 (1, 4, 5). Elevated enzymatic activity of aldehyde dehydrogenase (ALDH) or ganglioside synthase GD3S is also observed in cancer cells with CSC phenotype (6, 7). Despite progress in identifying CSC-associated markers, functional relevance of many of these markers remains to be characterized. The majority of signaling molecules that confer CSC phenotype to cancer cells are not cell surface molecules that can be used for therapeutic targeting (8). Among non-cell surface receptors enriched in CSCs, only GD3S is a therapeutic target (7). In this study, we demonstrate anthrax toxin receptor 1 (ANTXR1) as a functional CSC marker.

ANTXR1, a trans-membrane protein, is encoded by highly conserved *tumor endothelial marker 8* gene (9, 10). The cleaved C5A fragment of Collagen VI α3 serves as its physiological ligand (11). ANTXR1 interacts with lipoprotein receptor-related protein 6 (LRP6) and vascular endothelial growth factor receptor 2 and modulates signaling downstream of Wnt and VEGF, respectively (12–15). Furthermore, ANTXR1 is selectively expressed in tumor vasculature and promotes tumor angiogenesis (16, 17). Although ANTXR1 has previously been shown to be expressed in breast cancer cells (18), its functional role in these cells is unknown. This study provides evidence for its role in CSCs by activating Wnt signaling through its natural ligand. Since a subgroup of breast cancers contains a “reactive protein group” characterized by elevated levels of collagen VI (19) and missense mutations of Collagen VI α3 is observed in 6% of triple negative breast cancers (TNBCs) (20), we propose the existence of a cancer-specific signaling network involving ANTXR1 and Collagen VI, which impacts stemness phenotype.

Materials and Methods

Cell lines and plasmids

Breast cancer cell lines were purchased from ATCC and authenticated using STR Systems for Cell line identification (Promega, Madison, USA) by a commercial vender (DNAcenter.com) in August 2012. TMD-231 cells have been described previously (21). MCF-10A–ER-Src cells and the plasmid constructs bearing C5A, C5B, or C5C cDNAs were gifts from Dr. Kevin Struhl (Boston, MA, USA) and Dr. Brad Croix (Frederick, MD, USA), respectively. Supplementary information contains details of shRNA and siRNAs including catalogue numbers.

Flow cytometry sorting and analysis

MCF-10A Cells were incubated with FITC-conjugated CD44 and PE-conjugated CD24 antibody. Primary cells were incubated with FITC conjugated CD49f, APC conjugated EpCAM, and PE conjugated lineage markers CD31, CD45, and CD140b. Only lineage negative cells were sorted. Supplementary information has details of antibodies.

Mammosphere and invasion assays

One hundred thousand cells were seeded into ultralow adherent 100 mm plates (or 5000 cells in 6-well plate depending on the experiment) in MammoCult Medium (Stemcell Technologies, Vancouver, Canada). After 7–10 days of culturing, mammospheres were collected, resuspended in PBS, and large colonies were counted using a hemocytometer.

Alternatively, mammospheres were passed through a cell strainer (40 micron) and mammospheres blocked in the strainer were stained with Wright-Giemsa (Fisher Diagnostic, Middletown, VA, USA). For secondary and tertiary mammospheres, mammospheres were collected, trypsinized, and 5000 cells were replated in six well plates under mammosphere growth conditions. Invasion assay was performed using invasion assay kit (Millipore, Billerica, MA, USA).

RNA isolation, Microarray, Quantitative Reverse Transcription Polymerase Chain Reaction (qRT-PCR)

RNA was prepared using RNeasy kit (Qiagen, Valencia, CA, USA) and cDNA from two μg of RNA was synthesized using the cDNA Synthesis kit (Bio-Rad, Hercules, CA, USA). qRT-PCR was performed using SyberGreen on a TaqMan 7900HT instrument (Applied Biosystems, Carlsbad, CA, USA). Microarray with biological triplicates was performed using Illumina HumanHT-12 V4 expression beadchip. Genes differentially expressed at p value of <0.01 were considered for Ingenuity pathway and the transcription factor binding site (TFBS) enrichment analysis. Primers unique to ANTXR1 longest isoform were used for qRT-PCR analysis of primary tumor samples (primer sequences in the supplementary file).

Antibodies and Western blot analysis

Western blot analyses were done as described previously (22) and details of antibodies and recombinant proteins are provided in the supplementary information.

Animal model of breast cancer

The Institutional Animal Care and Utilization Committee approved all animal experiments. TMD-231 cells (10^6) with control shRNA vector or ANTXR1 shRNA were implanted into the mammary fat pad of 7-week-old female nude mice. Tumor volume was calculated using the formula: short dimension^2 × long dimension/2 (23). After 5-weeks, primary tumor and lungs were collected and subjected to Hematoxylin and Eosin (H&E) staining. A medical pathologist evaluated the slides in a single blinded manner and the metastasis index was calculated as described previously (23).

Results

ANTXR1 is a normal and cancer stem cell-enriched marker

Microarray analysis of CD44+/CD24− and CD44−/CD24+ subpopulation of immortalized cell line MCF-10A demonstrated significant differences in the expression of >2000 genes (22). Among differentially expressed genes, ANTXR1 drew our attention because this gene was previously considered functional mostly in tumor-associated endothelial cells (16). CD44+/CD24− cells expressed 4.2-fold higher levels of ANTXR1 compared to CD44−/CD24+ cells, which we further confirmed by western blot analysis (Fig. 1A). ANTXR1 expression in subpopulations of MCF-10A cells correlated positively with N-Cadherin but negatively with E-cadherin expression (22). To ascertain whether ANTXR1 is expressed at a higher level in specific subpopulation of cells from normal breast, we sorted primary cells into stem-cell enriched basal (CD49f+/EpCAM−/Lin−), bipotent/committed luminal progenitor (CD49f+/EpCAM+/Lin−), and mature luminal (CD49f−/EpCAM+/Lin−) cells (Fig. 1B) (24). Stem-cell enriched basal cells expressed highest levels of ANTXR1 compared to mature luminal cells (Fig. 1C). Analysis of gene expression array datasets from previous publications also demonstrated 3.2-fold and 13.5-fold higher ANTXR1 in stem-cell enriched basal cells compared to luminal progenitor or mature cells of human breast and murine mammary gland, respectively (25, 26).

We next examined ANTXR1 expression in primary breast tumors. ANTXR1 expression in representative tumors sorted based on Lin−, CD44±EpCAM or Lin−, CD49f±EpCAM is shown in Fig. 1D and 1E. CD44+/EpCAM− or CD49f+/EpCAM− cells expressed highest levels of ANTXR1 mRNA. To further demonstrate the presence of ANTXR1-positive primary cells, lineage-negative cells from normal breast or breast cancer were stained with an antibody that recognizes the extracellular domain of the longest isoform of ANTXR1. CD44+/ANTXR1+, CD44−/ANTXR1+, EpCAM+/ANTXR1+ and EpCAM−/ANTXR1+ cells are present in both normal breast and cancer (Fig. 1F). Primary CD49f+/ANTXR1+ cells expressed lower levels of myoepithelial/basal cell marker keratin 14 (K14) compared to CD49f+/ANTXR1− cells. This suggests that ANTXR1-positive cells either have lesser degree of myoepithelial differentiation or have features of epithelial to mesenchymal transition (EMT) (Fig. 1G).

A subpopulation of CD44−/CD24+ of MCF-10A cells engineered to overexpress the EMT-inducer Slug acquires CD44+/CD24− phenotype (22). This phenotypic conversion was associated with elevated expression of ANTXR1 at RNA levels (Fig. 1H) and cell surface protein levels (Fig. 1I). Unlike primary cells, ANTXR1-positive and ANTXR1-negative MCF-10A–Slug cells expressed similar levels of K14 (Fig. 1J), although K14 levels in MCF-10A–Slug cells were 50% lower than parental MCF-10A cells (data not shown).

Breast cancer subtype-specific prognostic relevance of ANTXR1

To determine the prognostic relevance of ANTXR1, we evaluated publicly available gene expression array datasets for ANTXR1 expression. In the Loi et al dataset (27), ANTXR1 overexpression correlated with poor recurrence free survival amongst patients with estrogen receptor (ER)-negative breast cancer (Fig. 2A). In Minn et al dataset (28), elevated ANTXR1 expression correlated with shorter distant metastasis-, lung metastasis-, and brain metastasis-free survival of patients with ER-negative and Progesterone Receptor (PR)-negative breast cancer (Fig. 2B–F). Overall, ANTXR1 overexpression is associated with poor outcome in ER-negative breast cancers, which are usually enriched for CD44+/CD24− CSCs (29). Additionally, in a dataset containing gene expression data of 478 patients with basal breast cancer (30), highest ANTXR1 (upper quartile) correlated with early recurrence (Fig. 2G).

We used Oncomine to analyze ANTXR1 copy number and expression changes in breast cancer compared to adjoining normal tissue. In the TCGA dataset (19), medullary carcinomas displayed ANTXR1 gene amplification (Supplementary Fig. 1A). ANTXR1 expression was elevated in ER-negative breast cancers compared to normal or ER-positive breast cancer (Supplementary Fig. 1B). PR-negative breast cancers also displayed elevated ANTXR1 levels compared to PR-positive tumors (data not shown). ERBB2-positive breast cancers overexpressed ANTXR1 compared to ERBB2-negative breast cancers (Supplementary Fig. 1C). TNBCs also displayed higher ANTXR1 expression than other breast cancer subtypes (Supplementary Fig. 1D). In addition, ANTXR1 is one among the top 10% overexpressed genes in five different breast cancer datasets present in the Oncomine database.

C5A, the natural ligand of ANTXR1, activates Wnt signaling

The above results prompted us to investigate ANTXR1 activated signals upon ligand stimulation. We selected five cell types for these studies; MCF-10A, SRC transformed MCF-10A (10A–SRC), parental MDA-MB-231 (MD-231), a variant of MD-231 isolated from a mammary fat pad tumor in nude mice (TMD-231), and SUM149 cells (21, 31). At least two ligands are known to activate ANTXR1; the PA antigen of anthrax and the C5A fragment of collagen VI α3 (11, 12, 32). Additionally, anthrax is thought to utilize the

ANTXR1 along with the Wnt receptor LRP6 for entry, although these results remain controversial (12, 33). ANTXR1 has previously been shown to respond to Wnt ligands (15); however, the ability of its natural ligand C5A to engage in Wnt pathway has not been demonstrated. Vector transfected or C5A transfected 10A–SRC cells were stimulated with PA antigen, Wnt3a, or both and were examined for the Wnt pathway target phospho-GSK3α/β. As expected, Wnt3a increased GSKα/β phosphorylation, whereas PA antigen marginally increased phospho-GSK3α/β (Fig. 3A). C5A transfected cells showed elevated basal phosphorylation of GSKα/β with no further increase in phosphorylation upon PA or Wnt3a addition (Fig. 3B). Similar studies were also performed in MCF-10A cells transiently transfected with C5A, C5B (functionally active variant of C5A), and C5C, an inactive variant that cannot bind to ANTXR1 (11). Transfected C5A and C5C generated secreted proteins (Fig. 3C). C5A and C5B but not C5C increased phospho-GSKα/β (Fig. 3B). C5A and C5B increased AXIN1, a feedback negative regulator of Wnt signaling. Wnt3a and PA antigen did not further increase AXIN1 expression or phospho-GSK3α/β in cells expressing C5A suggesting that these molecules compete for the same cell surface receptors (Fig. 3B).

AXIN2 and MSX2 are major Wnt target genes active in stem and cancer cells. AXIN2 expressing cells (AXIN2+) are described as Wnt-responsive bipotent stem cell subpopulation of adult mammary gland and these AXIN2+ cells contribute differently to basal and luminal lineages depending on developmental stages (34). MSX2 is an oncogene (35). Interestingly, C5A but not PA or Wnt3a increased AXIN2, whereas only Wnt3a increased the expression of MSX2 (Fig. 3D). Combined treatment with C5A and Wnt3a caused significantly higher expression of MSX2. To further demonstrate the requirement of Wnt pathway receptors for ANTXR1:C5A activated signals, we treated parental and C5A overexpressing cells with DKK, a natural antagonist of Wnt receptors (36). DKK treatment reduced phospho-GSK3α/β levels in C5A overexpressing cells (Fig. 3E). Collectively, these results demonstrate a functional crosstalk between C5A and Wnt pathway through ANTXR1. Mining for coexpression using BIIT (37) or Oncomine revealed several collagens including collagen VI α3 and MMP11, which is required for generating C5A (38), among top 50 genes coexpressed with ANTXR1 in multiple datasets. Thus, tumors are likely equipped with ANTXR1-MMP11-Collagen regulatory loop that aids in Wnt pathway activation.

ALDEFLUOR-positive breast cancer cells are enriched for ANTXR1 expression

To further extend an association between ANTXR1 and CSC phenotype, we sorted SUM149 cells into ALDEFLUOR-positive and ALDEFLUOR-negative subfractions (Fig. 4A). This cell line also has CD44+/CD24− and CD44+/CD24+ subfractions (Fig. 4B). ANTXR1 expression was higher in ALDEFLOUR-positive cells compared to ALDEFLOUR-negative cells (Fig. 4C). Similarly, CD44+/CD24− cells contained higher ANTXR1 compared to CD44+/CD24+ cells. ANTXR1 levels correlated positively with LRP6 and phospho-GSK3α/β levels. Taken together, these results show an association between ANTXR1 expression and previously established CSC phenotype of breast cancer cells.

ANTXR1 regulates LRP6 and Wnt target genes

To functionally link ANTXR1 with Wnt pathway activation, we generated MD-231 and TMD-231 cells expressing shRNA against ANTXR1 using retrovirus (Fig. 5A) and a lentivirus expression system with three independent siRNAs (Fig. 5B). Another set of ANTXR1-specific siRNA was used for transient knockdown of ANTXR1 in SUM149 and TMD-231 cells (Fig. 5C). The effects of si/shRNA on ANTXR1 mRNA levels are shown in Fig. 5D. ANTXR1 knockdown resulted in reduced expression of Wnt pathway-associated proteins including LRP6, AXIN1, ZEB1, cMyc, phospho-GSK3α/β, and Cyclin D1 compared to control cells (Fig. 5A–C). ANTXR1 knockdown also altered phospho-

ERK1:ERK2 ratio (Fig. 5A). Note that ANTXR1 knockdown had no effect on survivin expression suggesting specificity in ANTXR1 pathway (Fig. 5A). ANTXR1 is likely constitutively active in these cells because microarray results showed Collagen VI α3 expression in TMD-231 cells (data not shown).

The observation of lower LRP6 in ANTXR1 knockdown cells is interesting as LRP6 is one of the Wnt receptor (13). To confirm ANTXR1 directly targets LRP6, we measured LRP6 mRNA levels by qRT-PCR. ANTXR1 knockdown cells displayed lower LRP6 mRNA compared to vector control cells (Fig. 5E). Therefore, ANTXR1 may directly regulate Wnt pathway by controlling the expression of LRP6.

We subjected TMD-231 cells with control and ANTXR1 shRNAs to Wnt pathway specific array and a global microarray. Wnt pathway specific array identified BMP4 as an ANTXR1 target gene. QRT-PCR assay showed higher levels of BMP4 in control cells compared to ANTXR1 knockdown cells (Fig. 5F). Microarray analysis showed differential expression of 659 genes ($P<0.01$, Table S1); 165 genes were downregulated in ANTXR1 shRNA cells compared to control shRNA cells. Ingenuity pathway analysis identified three ANTXR1-associated signaling networks (Supplementary Fig. 2A–C). β-Catenin and cMyc were integral part of these networks highlighting an association between ANTXR1, Wnt pathway, and the stemness phenotype. TFBS enrichment analysis of the regulatory regions of differentially expressed genes linked ANTXR1 signaling to transcription regulation by Transcription Factor EB (TFEB), Nuclear Factor Erythroid derived 2 (NF-E2), SMAD member 4 (SMAD4), GA Binding Protein transcription factor, Beta subunit 1 (GABPB1), Androgen Receptor (AR), and Heat Shock Transcription Factor 2 (HSF2) ($p<4.3$ E-02).

Gene expression array results indicated additional ANTXR1 targets linked to CSC and metastasis. For example, the levels of HSPB1, which helps to switch dormant tumors to aggressive phenotype (39), were lower in ANTXR1 knockdown cells (Table S1). The levels of HSPA1A, which is overexpressed in the metastatic TNBC CSCs (40), were 3-fold lower in ANTXR1 knockdown cells compared to control cells. Indeed, qRT-PCR assay confirmed the results of microarray results (Fig. 5G). Parental MD-231 cells expressed much lower HSPA1A compared to TMD-231 and its expression was unaffected upon ANTXR1 knockdown. In contrast to lower HSPA1A, TMD-231 cells expressing ANTXR1 shRNA demonstrated elevated expression of luminal epithelial cell enriched genes such as FOXA1, LRIG1, and TFAP2C (Table S1). In fact, Ingenuity pathway analysis of ANTXR1 shRNA cell-enriched genes showed ER network (Supplementary Fig. 3A). Although ANTXR1 knockdown in TMD-231 cells did not result in ER expression (data shown), FOXA1 expression was increased in knockdown cells (Fig. 5A). FOXA1 influences ERα expression, function, ductal morphogenesis, and is a good prognostic marker of breast cancer (41, 42). These results demonstrate a link between ANTXR1, Wnt pathway, and the metastasis-associated HSPA1A expression as well as the ability of ANTXR1 signaling to suppress luminal cell-enriched gene network.

To extend a link between ANTXR1 and HSPA1A to primary tumors, we analyzed prognostic significance of ANTXR1 and HSPA1A expression using a public database (30). Patients expressing elevated levels of ANTXR1 and HSPA1A demonstrated worst recurrence-free, distant metastasis-free and overall survival (Supplementary Fig. 3). Elevated ANTXR1+ HSPA1A expression also correlated with poor recurrence-free and metastasis-free survival of patients who did not receive systemic therapy.

ANTXR1:C5A axis promotes stem cell-like phenotype

To evaluate whether ANTXR1-induced signaling in human breast epithelial cells exert a stem cell-enriched function, MCF-10A with control vector or overexpressing C5A were

subjected to mammosphere assay to assess stem cell function and to flow cytometry to measure stem cell-enriched basal markers. Although legitimacy of mammosphere assay for stem cell function is debated, it is at least considered to measure anoikis resistance capabilities. MCF-10A vector control cells formed fewer and smaller mammospheres (Fig. 6A). In contrast, C5A transfected cells formed much larger and more (> 5 fold) mammospheres (Fig. 6A). In addition, C5A overexpressing cells compared to control cells showed elevated expression of CD44 (Fig. 6B).

We examined TMD-231 cells expressing ANTXR1 shRNA for reversal of stem cell features. Most of the breast CSCs shows mesenchymal phenotype as evident from their elongated morphology with very little cell-cell contact (8, 43). TMD-231 cells with control shRNA displayed this morphology (Fig. 6C). In contrast, TMD-231 cells expressing ANTXR1 shRNA grew in clusters with cell-cell contact and morphological features of epithelial cells. Furthermore, ANTXR1 shRNA expressing cells formed fewer and smaller mammospheres compared to cells with control shRNA (Fig. 6D). ANTXR1 knockdown increased cell surface levels of EpCAM, epithelial/luminal cell-enriched molecule (Fig. 6E).

To ensure that observed mammospheres are not just cell aggregates, we plated single cell in ultra-low adherent 96 well plates using flow cytometry sorter. Mammospheres developed in few but not all wells (Supplementary Fig. 4A). We also measured the ability of vector control and ANTXR1 knockdown cells to generate secondary and tertiary mammospheres. Size as well as number of secondary and tertiary mammospheres remained low with ANTXR1 knockdown cells compared to parental cells (Supplementary Fig. 4B and 4C).

To further associate ANTXR1 with CSC phenotype, we sorted ANTXR1-positive and negative cells from TMD-231 cells and examined for their ability to form mammospheres. Cells used in this experiment can be categorized as CD44+/CD24−/ANTXR1+ and CD44+/CD24−/ANTXR1− cells because close to 100% of TMD-231 cells are CD44+/CD24− (43). ANTXR1-positive cells compared to ANTXR1-negative cells formed larger and increased number of mammospheres (Supplementary Fig. 4D). Thus, CD44+/CD24−/ANTXR1+ cells represent a distinct population of CSCs with higher self-renewal capacity.

ANTXR1 accelerates tumor growth and lung metastasis

To determine whether ANTXR1 expression affects malignant behavior of cancer cells *in vivo*, we injected TMD-231 cells with control shRNA or ANTXR1 shRNA into the mammary fat pad of nude mice. Unlike parental MD-231 cells, TMD-231 cells injected into the mammary fat pad spontaneously metastasize to lungs. Tumors formed by ANTXR1 shRNA cells were significantly smaller compared to tumors derived from control shRNA cells (Fig. 7A). However, histologically, tumors between two groups did not show significant differences (Supplementary Fig. 5A). Furthermore, both TMD231 control shRNA and ANTXR1 shRNA cells grew at similar rate in 2D cultures (Supplementary Fig. 5B). Therefore, differences in growth rate in vivo could be related to differences in stemness phenotype and the ability to establish and/or respond to a proper tumor microenvironment. We do note limitation of our assay, as limited dilution mammary fat pad implantation is required to fully establish relationship between ANTXR1-dependent stemness phenotype and tumorigenicity.

Lungs after five weeks of tumor cell implantation showed extensive metastasis in animals injected with TMD-231 control shRNA compared to ANTXR1 shRNA cells (Fig. 7B). Representative H&E staining of lungs from two different groups is shown in Fig. 7C. Reduced lung metastasis of ANTXR1 knockdown cells could be related to lower invasive capacity of these cells or due to inability to home and grow in lungs. Since we had previously demonstrated that CSC (CD44+/CD24−) phenotype is associated with increased

invasive capacity but not homing and growth in lungs (43), and ANTXR1 knockdown reversing some of the EMT features, we examined whether ANTXR1 knockdown reduces invasive capacity using matrigel invasion assay. Indeed, ANTXR1 knockdown cells showed reduced invasion compared to vector control cells, suggesting that ANTXR1 is required for invasion of cancer cells (Fig. 7D).

In an independent experiment with same clones but higher passage number in culture (lower ANTXR1 knockdown), tumor growth differences persisted even at eight weeks; however, differences in metastasis rate were not statistically significant at this later time point (Supplementary Fig. 6). These findings indicate that ANTXR1 plays a substantial role in driving breast cancer growth and metastasis and its effective inhibition delays metastasis.

Discussion

ANTXR1 has been studied extensively in the context of tumor vasculature. Antibodies against its extracellular domain reduced tumor-induced angiogenesis and increased sensitivity of variety of tumors to anticancer agents (16). However, the degree of ANTXR1 dependence for tumor growth and drug response varied among different cancer types, and did not correlate with ANTXR1 expression in cancer-associated endothelial cells (16). In light of our discovery, we propose that the tumor-specific differences in CSCs expressing ANTXR1 determine the sensitivity to ANTXR1-targeting antibodies. Although previous reports have indicated ANTXR1 expression in breast cancer cells and its expression correlating with shorter survival outcome (44), cell types within breast cancer or normal breast that express ANTXR1 are not known. Our study addresses this issue as well as delineates signaling pathways downstream of ANTXR1. ANTXR1 expression was observed predominantly in basal-like cell lines and in few luminal cell lines (data not shown) and had prognostic impact in ERα-negative/basal breast cancers. Iyengar et al recently demonstrated that adipocyte-derived carboxy terminal fragment of collagen VI α3 activates AKT and β-Catenin and promotes breast cancer progression by serving as a ligand for NG2/chondroitin sulphate proteoglycan receptor expressed on cancer cells (45). Our study identified a distinct pathway activated by the carboxy terminus of Collagen VI α3 through ANTXR1. Since stromal fibroblasts produce MMP11, which is essential for cleavage of collagen VI (38), a three-way communication between cancer cells, adipocytes, and fibroblasts may influence stem cell-enriched gene expression program in cancer cells. Recent publication by cancer genome atlas network supports this possibility as a subgroup of breast cancers contains distinct “reactive group”, which is enriched for collagen VI (19). Further relevance of collagen VI α3 in breast cancer is evident from genome-wide sequencing studies as missense mutation affecting this gene is observed in 6% of TNBCs (20). Furthermore, coexpression analysis using Oncomine reinforces the existence of a network comprising ANTXR1, MMP11, and Collagens within the tumor microenvironment. This network may be an ideal therapeutic target.

Previous studies demonstrated physical association between LRP6 and ANTXR1 and the influence of this association on Wnt pathway (12, 13, 46). Our results demonstrate an additional link as ANTXR1-mediated signaling directly controlled the mRNA levels of LRP6 (Fig. 5). Gene expression array analysis of control and ANTXR1 knockdown cells clearly indicated the effects of ANTXR1 knockdown on transcription factor signaling network including Wnt, JNK/AP1, and E2F (Supplementary Fig. 2A–C). LRP6 regulatory regions contain AP1 and E2F binding sites and ANTXR1 may utilize these transcription factors to control LRP6 expression.

Our results described in Fig. 5A–C showed ZEB1 as another critical target of ANTXR1. This ANTXR1:ZEB1 axis has implications on sensitivity of cancer cells to targeted

therapies. A recent synthetic lethal interaction study showed elevated expression of ANTXR1 correlating with lack of response to combined MEK and BCL-XL inhibitors and sensitivity to this combination could be regained upon ZEB1 knockdown (47). Since ZEB1 is a master regulator of mesenchymal differentiation and one of the regulators of CSC phenotype (48), ANTXR1 may control CSC phenotype as well as sensitivity to targeted therapy through ZEB1, which will be the subject of future investigation.

Based on the expression pattern, it appears that ANTXR1 controls signaling in stem/progenitor cells of both normal and cancerous breast. In cancer, these pathways include β-catenin, cMyc, TGFβ/SMAD, and JNK (Supplementary Fig. 2). While first three pathways are associated with CSC phenotype, inactivation of JNK pathway is associated with breast cancer initiation/progression (49, 50). Results of these pathway analyses coupled with direct demonstration of the effects of ANTXR1 on the expression of LRP6, ZEB1, mammosphere formation, tumor growth, invasion, and metastasis provide strong evidence for ANTXR1 as a functional marker of cancer stem cells. Moreover, it is believed that CD44+/CD24− cells are enriched in basal breast cancers, whereas ALDEFLUOR-positive cells are enriched in luminal breast cancers. Therefore, targeting ANTXR1 would be beneficial for CSC-enriched both basal and luminal breast cancers. However, success of ANTXR1-targeted therapies will depend on which among pathways downstream of ANTXR1 the cancer cells are addicted to and are amicable to therapeutic intervention. If cancer cells addicted to ANTXR1 signaling are CSCs as this study indicates, ANTXR1 targeted therapies can potentially limit intratumoral heterogeneity. Furthermore, since ANTXR1 is expressed in hematopoietic and endothelial cells, therapies targeting ANTXR1 would limit the impact of tumor microenvironment on CSC features and heterogeneity.

Supplementary Material

Refer to Web version on PubMed Central for supplementary material.

Acknowledgments

Funding support: NIH grant R21 CA152536-01A1 and Susan Komen for the Cure grant SAC110025 to HN.

We thank Drs. Kevin Struhl, Brad Croix, and Stephen Leppla for reagents and advise. We also thank IUSCC flow cytometry core for flow cytometry and the Breast Cancer Signature Center-IU Simon Cancer Center at Indiana University-Purdue University, Indianapolis for the database of publicly available microarray data.

References

1. Pece S, Tosoni D, Confalonieri S, Mazzarol G, Vecchi M, Ronzoni S, et al. Biological and molecular heterogeneity of breast cancers correlates with their cancer stem cell content. Cell. 2010; 140:62–73. [PubMed: 20074520]
2. Badve S, Nakshatri H. Breast-cancer stem cells-beyond semantics. Lancet Oncol. 2012; 13:e43–e48. [PubMed: 22225725]
3. Nguyen LV, Vanner R, Dirks P, Eaves CJ. Cancer stem cells: an evolving concept. Nat Rev Cancer. 2012; 12:133–143. [PubMed: 22237392]
4. Al-Hajj M, Wicha MS, Benito-Hernandez A, Morrison SJ, Clarke MF. Prospective identification of tumorigenic breast cancer cells. Proc Natl Acad Sci U S A. 2003; 100:3983–3988. [PubMed: 12629218]
5. Kim J, Villadsen R, Sorlie T, Fogh L, Gronlund SZ, Fridriksdottir AJ, et al. Tumor initiating but differentiated luminal-like breast cancer cells are highly invasive in the absence of basal-like activity. Proc Natl Acad Sci U S A. 2012; 109:6124–6129. [PubMed: 22454501]
6. Ginestier C, Hur MH, Charafe-Jauffret E, Monville F, Dutcher J, Brown M, et al. ALDH1 Is a Marker of Normal and Malignant Human Mammary Stem Cells and a Predictor of Poor Clinical Outcome. Cell Stem Cell. 2007; 1:555–567. [PubMed: 18371393]

7. Battula VL, Shi Y, Evans KW, Wang RY, Spaeth EL, Jacamo RO, et al. Ganglioside GD2 identifies breast cancer stem cells and promotes tumorigenesis. J Clin Invest. 2012; 122:2066–2078. [PubMed: 22585577]
8. Mani SA, Guo W, Liao MJ, Eaton EN, Ayyanan A, Zhou AY, et al. The epithelial-mesenchymal transition generates cells with properties of stem cells. Cell. 2008; 133:704–715. [PubMed: 18485877]
9. St Croix B, Rago C, Velculescu V, Traverso G, Romans KE, Montgomery E, et al. Genes expressed in human tumor endothelium. Science. 2000; 289:1197–1202. [PubMed: 10947988]
10. Bradley KA, Mogridge J, Mourez M, Collier RJ, Young JA. Identification of the cellular receptor for anthrax toxin. Nature. 2001; 414:225–229. [PubMed: 11700562]
11. Nanda A, Carson-Walter EB, Seaman S, Barber TD, Stampfl J, Singh S, et al. TEM8 interacts with the cleaved C5 domain of collagen alpha 3(VI). Cancer Res. 2004; 64:817–820. [PubMed: 14871805]
12. Wei W, Lu Q, Chaudry GJ, Leppla SH, Cohen SN. The LDL receptor-related protein LRP6 mediates internalization and lethality of anthrax toxin. Cell. 2006; 124:1141–1154. [PubMed: 16564009]
13. Abrami L, Kunz B, Deuquet J, Bafico A, Davidson G, van der Goot FG. Functional interactions between anthrax toxin receptors and the WNT signalling protein LRP6. Cellular microbiology. 2008; 10:2509–2519. [PubMed: 18717822]
14. Jinnin M, Medici D, Park L, Limaye N, Liu Y, Boscolo E, et al. Suppressed NFAT-dependent VEGFR1 expression and constitutive VEGFR2 signaling in infantile hemangioma. Nat Med. 2008; 14:1236–1246. [PubMed: 18931684]
15. Verma K, Gu J, Werner E. Tumor endothelial marker 8 amplifies canonical Wnt signaling in blood vessels. PloS one. 2011; 6:e22334. [PubMed: 21829615]
16. Chaudhary A, Hilton MB, Seaman S, Haines DC, Stevenson S, Lemotte PK, et al. TEM8/ANTXR1 blockade inhibits pathological angiogenesis and potentiates tumoricidal responses against multiple cancer types. Cancer Cell. 2012; 21:212–226. [PubMed: 22340594]
17. Werner E, Kowalczyk AP, Faundez V. Anthrax toxin receptor 1/tumor endothelium marker 8 mediates cell spreading by coupling extracellular ligands to the actin cytoskeleton. J Biol Chem. 2006; 281:23227–23236. [PubMed: 16762926]
18. Gutwein LG, Al-Quran SZ, Fernando S, Fletcher BS, Copeland EM, Grobmyer SR. Tumor endothelial marker 8 expression in triple-negative breast cancer. Anticancer Res. 2011; 31:3417–3422. [PubMed: 21965755]
19. Koboldt DC, Fulton RS, McLellan MD, Schmidt H, Kalicki-Veizer J, McMichael JF, et al. Comprehensive molecular portraits of human breast tumours. Nature. 2012
20. Shah SP, Roth A, Goya R, Oloumi A, Ha G, Zhao Y, et al. The clonal and mutational evolution spectrum of primary triple-negative breast cancers. Nature. 2012; 486:395–399. [PubMed: 22495314]
21. Helbig G, Christopherson KW 2nd, Bhat-Nakshatri P, Kumar S, Kishimoto H, Miller KD, et al. NF-kappaB promotes breast cancer cell migration and metastasis by inducing the expression of the chemokine receptor CXCR4. J Biol Chem. 2003; 278:21631–21638. [PubMed: 12690099]
22. Bhat-Nakshatri P, Appaiah H, Ballas C, Pick-Franke P, Goulet R Jr, Badve S, et al. SLUG/SNAI2 and tumor necrosis factor generate breast cells with CD44+/CD24− phenotype. BMC cancer. 2010; 10:411. [PubMed: 20691079]
23. Sweeney CJ, Mehrotra S, Sadaria MR, Kumar S, Shortle NH, Roman Y, et al. The sesquiterpene lactone parthenolide in combination with docetaxel reduces metastasis and improves survival in a xenograft model of breast cancer. Mol Cancer Ther. 2005; 4:1004–1012. [PubMed: 15956258]
24. Visvader JE. Keeping abreast of the mammary epithelial hierarchy and breast tumorigenesis. Genes Dev. 2009; 23:2563–2577. [PubMed: 19933147]
25. Lim E, Vaillant F, Wu D, Forrest NC, Pal B, Hart AH, et al. Aberrant luminal progenitors as the candidate target population for basal tumor development in BRCA1 mutation carriers. Nat Med. 2009; 15:907–913. [PubMed: 19648928]

26. Lim E, Wu D, Pal B, Bouras T, Asselin-Labat ML, Vaillant F, et al. Transcriptome analyses of mouse and human mammary cell subpopulations reveal multiple conserved genes and pathways. Breast Cancer Res. 2010; 12:R21. [PubMed: 20346151]
27. Loi S, Haibe-Kains B, Desmedt C, Lallemand F, Tutt AM, Gillet C, et al. Definition of clinically distinct molecular subtypes in estrogen receptor-positive breast carcinomas through genomic grade. J Clin Oncol. 2007; 25:1239–1246. [PubMed: 17401012]
28. Minn AJ, Gupta GP, Siegel PM, Bos PD, Shu W, Giri DD, et al. Genes that mediate breast cancer metastasis to lung. Nature. 2005; 436:518–524. [PubMed: 16049480]
29. Creighton CJ, Li X, Landis M, Dixon JM, Neumeister VM, Sjolund A, et al. Residual breast cancers after conventional therapy display mesenchymal as well as tumor-initiating features. Proc Natl Acad Sci U S A. 2009; 106:13820–13825. [PubMed: 19666588]
30. Gyorffy B, Lanczky A, Eklund AC, Denkert C, Budczies J, Li Q, et al. An online survival analysis tool to rapidly assess the effect of 22,277 genes on breast cancer prognosis using microarray data of 1,809 patients. Breast Cancer Res Treat. 2010; 123:725–731. [PubMed: 20020197]
31. Iliopoulos D, Hirsch HA, Struhl K. An epigenetic switch involving NF-kappaB, Lin28, Let-7 MicroRNA, and IL6 links inflammation to cell transformation. Cell. 2009; 139:693–706. [PubMed: 19878981]
32. Abrami L, Kunz B, van der Goot FG. Anthrax toxin triggers the activation of src-like kinases to mediate its own uptake. Proc Natl Acad Sci U S A. 2010; 107:1420–1424. [PubMed: 20080640]
33. Young JJ, Bromberg-White JL, Zylstra C, Church JT, Boguslawski E, Resau JH, et al. LRP5 and LRP6 are not required for protective antigen-mediated internalization or lethality of anthrax lethal toxin. PLoS pathogens. 2007; 3:e27. [PubMed: 17335347]
34. van Amerongen RBA, Nusse R. Developmental stage and time dictate the fate of Wnt/beta-catenin-responsive stem cells in the mammary gland. Cell Stem Cell. 2012; 11:387–400. [PubMed: 22863533]
35. Zhai Y, Iura A, Yeasmin S, Wiese AB, Wu R, Feng Y, et al. MSX2 is an oncogenic downstream target of activated WNT signaling in ovarian endometrioid adenocarcinoma. Oncogene. 2011; 30:4152–4162. [PubMed: 21499300]
36. Katoh M, Katoh M. WNT signaling pathway and stem cell signaling network. Clin Cancer Res. 2007; 13:4042–4045. [PubMed: 17634527]
37. Adler P, Kolde R, Kull M, Tkachenko A, Peterson H, Reimand J, et al. Mining for coexpression across hundreds of datasets using novel rank aggregation and visualization methods. Genome Biol. 2009; 10:R139. [PubMed: 19961599]
38. Motrescu ER, Blaise S, Etique N, Messaddeq N, Chenard MP, Stoll I, et al. Matrix metalloproteinase-11/stromelysin-3 exhibits collagenolytic function against collagen VI under normal and malignant conditions. Oncogene. 2008; 27:6347–6355. [PubMed: 18622425]
39. Straume O, Shimamura T, Lampa MJ, Carretero J, Oyan AM, Jia D, et al. Suppression of heat shock protein 27 induces long-term dormancy in human breast cancer. Proc Natl Acad Sci U S A. 2012; 109:8699–8704. [PubMed: 22589302]
40. Kaur P, Nagaraja GM, Zheng H, Gizachew D, Galukande M, Krishnan S, et al. A mouse model for triple-negative breast cancer tumor-initiating cells (TNBC-TICs) exhibits similar aggressive phenotype to the human disease. BMC cancer. 2012; 12:120. [PubMed: 22452810]
41. Bernardo GM, Lozada KL, Miedler JD, Harburg G, Hewitt SC, Mosley JD, et al. FOXA1 is an essential determinant of ERalpha expression and mammary ductal morphogenesis. Development. 2010; 137:2045–2054. [PubMed: 20501593]
42. Badve S, Turbin D, Thorat MA, Morimiya A, Nielsen TO, Perou CM, et al. FOXA1 expression in breast cancer--correlation with luminal subtype A and survival. Clin Cancer Res. 2007; 13:4415–4421. [PubMed: 17671124]
43. Sheridan C, Kishimoto H, Fuchs RK, Mehrotra S, Bhat-Nakshatri P, Turner CH, et al. CD44+/CD24− breast cancer cells exhibit enhanced invasive properties: an early step necessary for metastasis. Breast Cancer Res. 2006; 8:R59. [PubMed: 17062128]
44. Davies G, Rmali KA, Watkins G, Mansel RE, Mason MD, Jiang WG. Elevated levels of tumour endothelial marker-8 in human breast cancer and its clinical significance. Int J Oncol. 2006; 29:1311–1317. [PubMed: 17016666]

45. Iyengar P, Espina V, Williams TW, Lin Y, Berry D, Jelicks LA, et al. Adipocyte-derived collagen VI affects early mammary tumor progression in vivo, demonstrating a critical interaction in the tumor/stroma microenvironment. J Clin Invest. 2005; 115:1163–1176. [PubMed: 15841211]

46. Kim HH, van den Heuvel AP, Schmidt JW, Ross SR. Novel common integration sites targeted by mouse mammary tumor virus insertion in mammary tumors have oncogenic activity. PloS one. 2011; 6:e27425. [PubMed: 22087314]

47. Corcoran RB, Cheng KA, Hata AN, Faber AC, Ebi H, Coffee EM, et al. Synthetic lethal interaction of combined BCL-XL and MEK inhibition promotes tumor regressions in KRAS mutant cancer models. Cancer Cell. 2013; 23:121–128. [PubMed: 23245996]

48. Brabletz S, Brabletz T. The ZEB/miR-200 feedback loop--a motor of cellular plasticity in development and cancer? EMBO Rep. 2010; 11:670–677. [PubMed: 20706219]

49. O'Brien CA, Kreso A, Jamieson CH. Cancer stem cells and self-renewal. Clin Cancer Res. 2010; 16:3113–3120. [PubMed: 20530701]

50. Stephens PJ, Tarpey PS, Davies H, Van Loo P, Greenman C, Wedge DC, et al. The landscape of cancer genes and mutational processes in breast cancer. Nature. 2012; 486:400–404. [PubMed: 22722201]

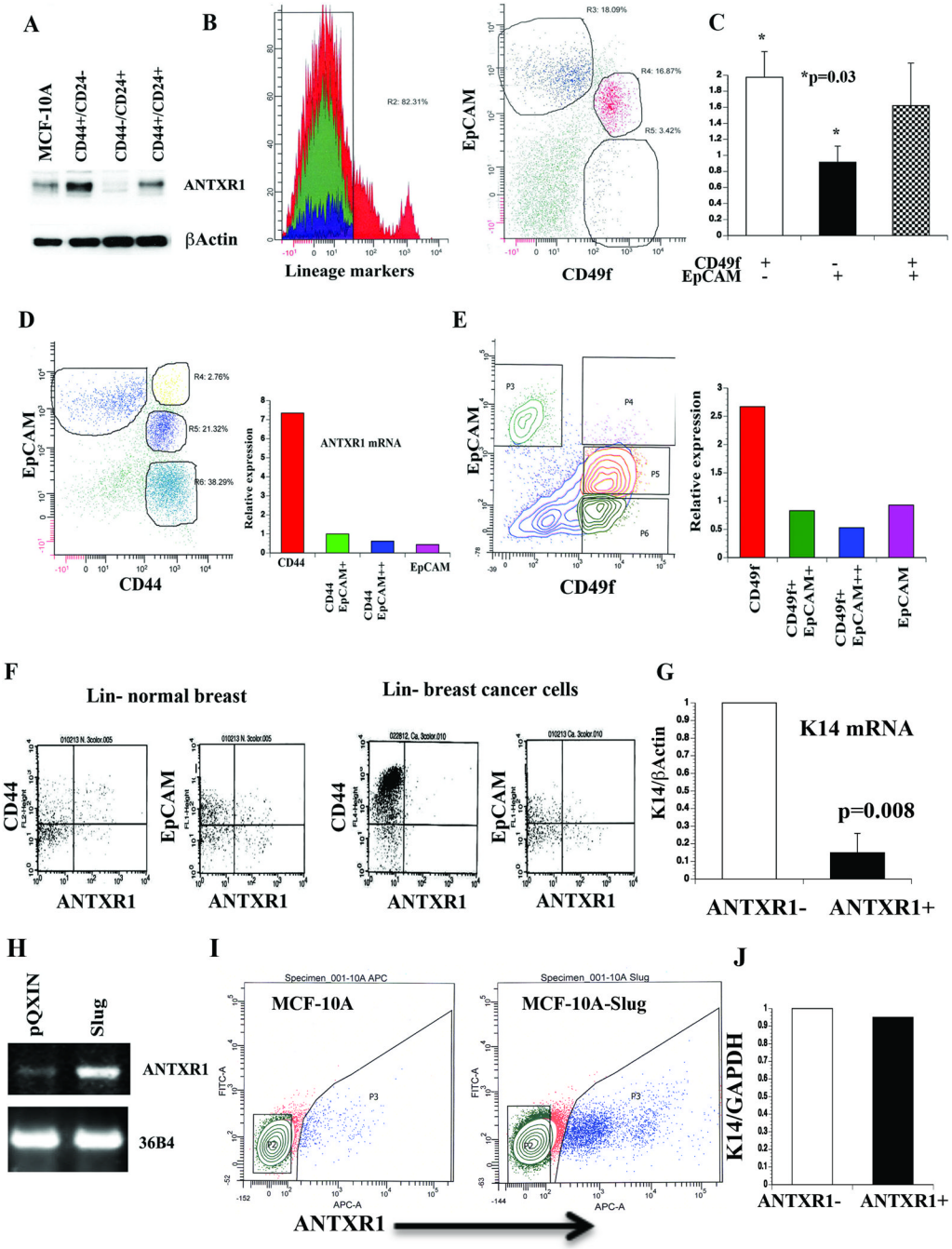

Fig. 1. Stem cell-enriched expression of ANTXR1

A) CD44+/CD24− subpopulation of MCF-10A cells expresses higher levels of ANTXR1 compared to unsorted cells or CD44−/CD24+ cells. B) Representative FACS dotplot profile of normal breast cells stained with CD49f, EpCAM, and Lineage marker antibodies. Stem cell-enriched basal (CD49f+/EpCAM−/Lin−), luminal progenitor cell enriched (CD49f+/EpCAM+/Lin−) and mature cell (CD49f−/EpCAM+/Lin−) fractions (25, 26) were sorted for mRNA preparation. C) Stem cell-enriched basal cell fraction contains higher levels of ANTXR1 mRNA compared to mature cells (N=4, Average ± standard error, *p=0.03). D) CD44+/EpCAM− primary breast tumor cells express highest level of ANTXR1. A typical flow cytometry profile of lineage-negative cancer cells stained for CD44 and EpCAM is

shown in left, and qRT-PCR results of ANTXR1 expression are shown in right. E) CD49f+/EpCAM- primary tumor cells express highest level of ANTXR1. F) Cell surface expression of ANTXR1. Lineage-negative primary normal or cancerous breast cells were stained with ANTXR1 and CD44 or EpCAM. G) Keratin 14 (K14) expression in ANTXR1-negative and ANTXR1-positive primary CD49f+/EpCAM- breast epithelial cells (n=2). H) MCF-10A cells undergoing EMT upon Slug overexpression show elevated ANTXR1. A representative RT-PCR data along with 36B4 as a control is shown. I) Cell surface ANTXR1 levels in parental MCF-10A and MCF-10A–Slug cells. J) K14 mRNA levels in ANTXR1-positive and ANTXR1-negative MCF-10A–Slug cells.

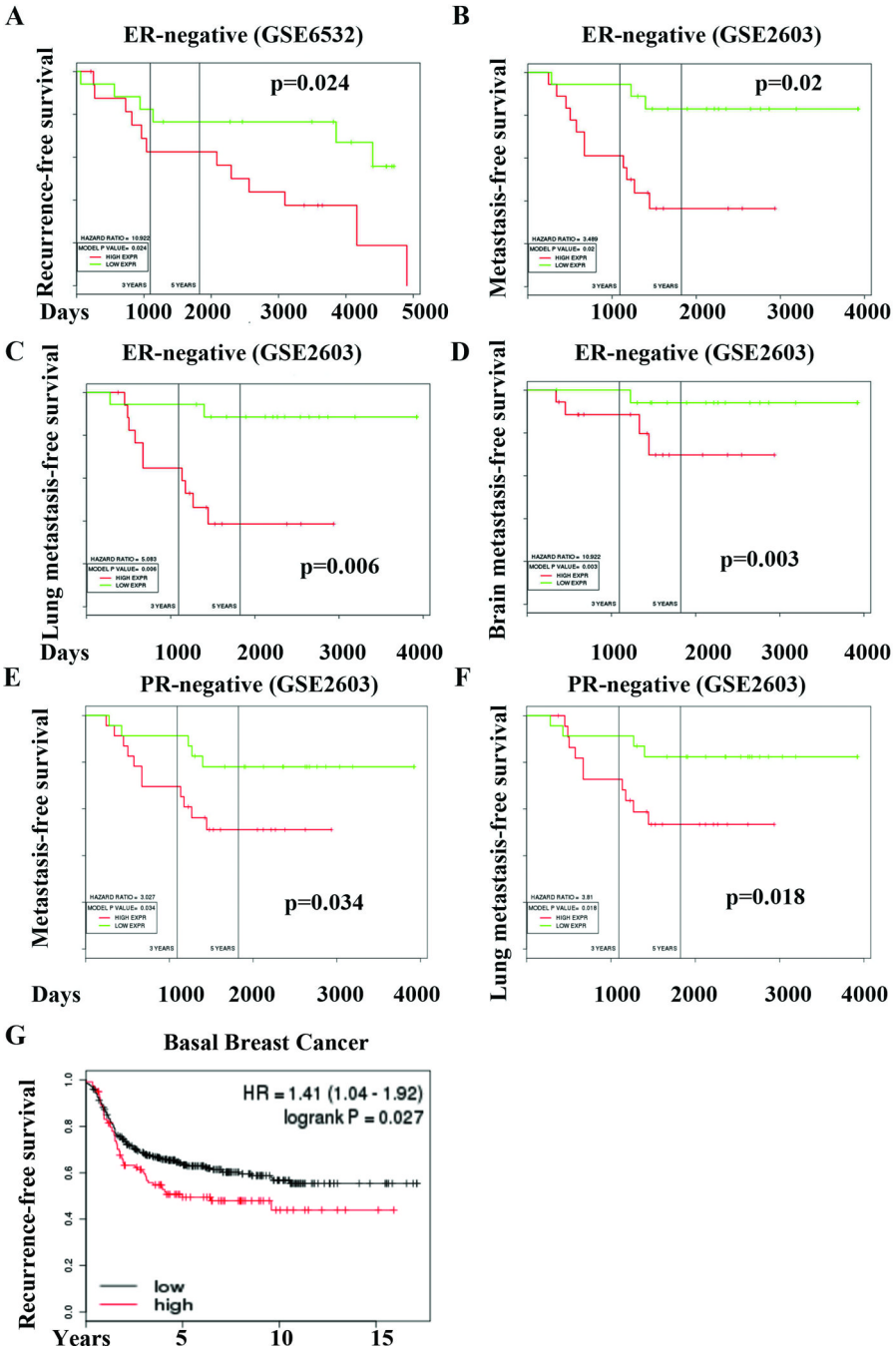

Fig. 2. Prognostic significance of ANTXR1

A) Kaplan-Meir plot (KM) displaying recurrence-free survival of ER-negative breast cancer patients with tumors expressing high (red) or low (green) levels of ANTXR1 mRNA. In a different dataset, ANTXR1 expression is associated with unfavorable metastasis-free (B), lung metastasis-free (C), brain metastasis-free (D) survival in ER-negative patients and in PR-negative patients (E and F). G) Recurrence-free survival of patients with basal breast cancer expressing high (red) or low (black) levels of ANTXR1.

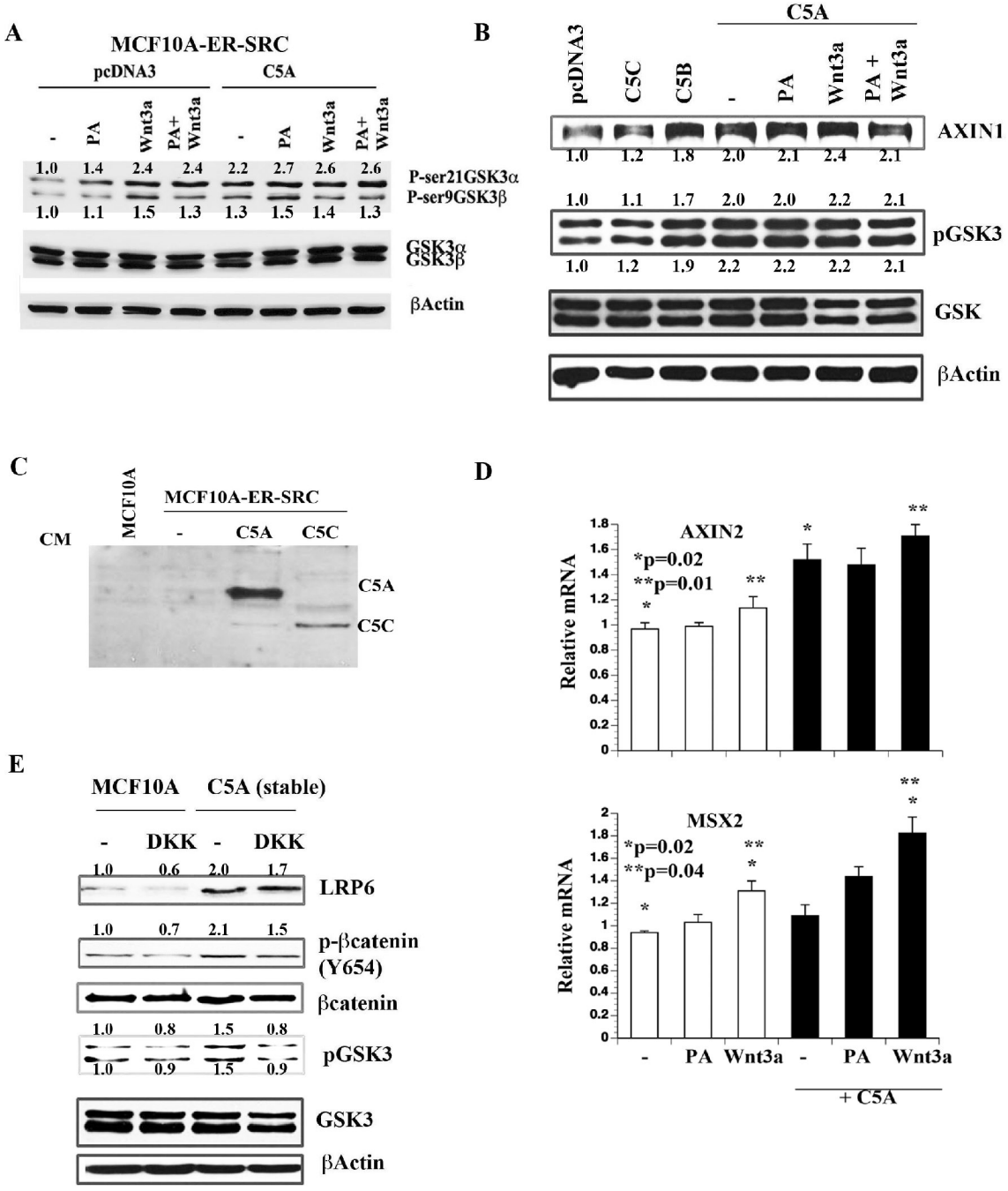

Fig. 3. C5A activates Wnt signaling pathway

A) The effect of C5A overexpression on GSK3 phosphorylation in MCF-10A–ER-SRC cells. Cells were transiently transfected with pcDNA3 or C5A for 24 hours and then treated with PA antigen (500 ng/ml) or Wnt3a (100 ng/ml) for 24 hours. B) C5A and C5B but not C5C activate Wnt signaling. Experiments were done as in A in MCF-10A cells. C) C5A and C5C are secreted proteins. Conditioned media from MCF-10A–ER-SRC cells transfected with C5A or C5C were concentrated and analyzed for C5A or C5C with cMyc tag antibody. D) The effect of C5A, PA, and Wnt3a on expression of genes downstream of Wnt signaling in MCF-10A cells. Experiments were performed as in B and mRNA levels were measured by qRT-PCR (Average ±standard error). E) MCF-10A cells stably expressing C5A show

Wnt pathway activation, which can be partially suppressed by DKK. Cells were treated with DKK (20 ng/ml) overnight and analyzed by Western blot with indicated antibodies.

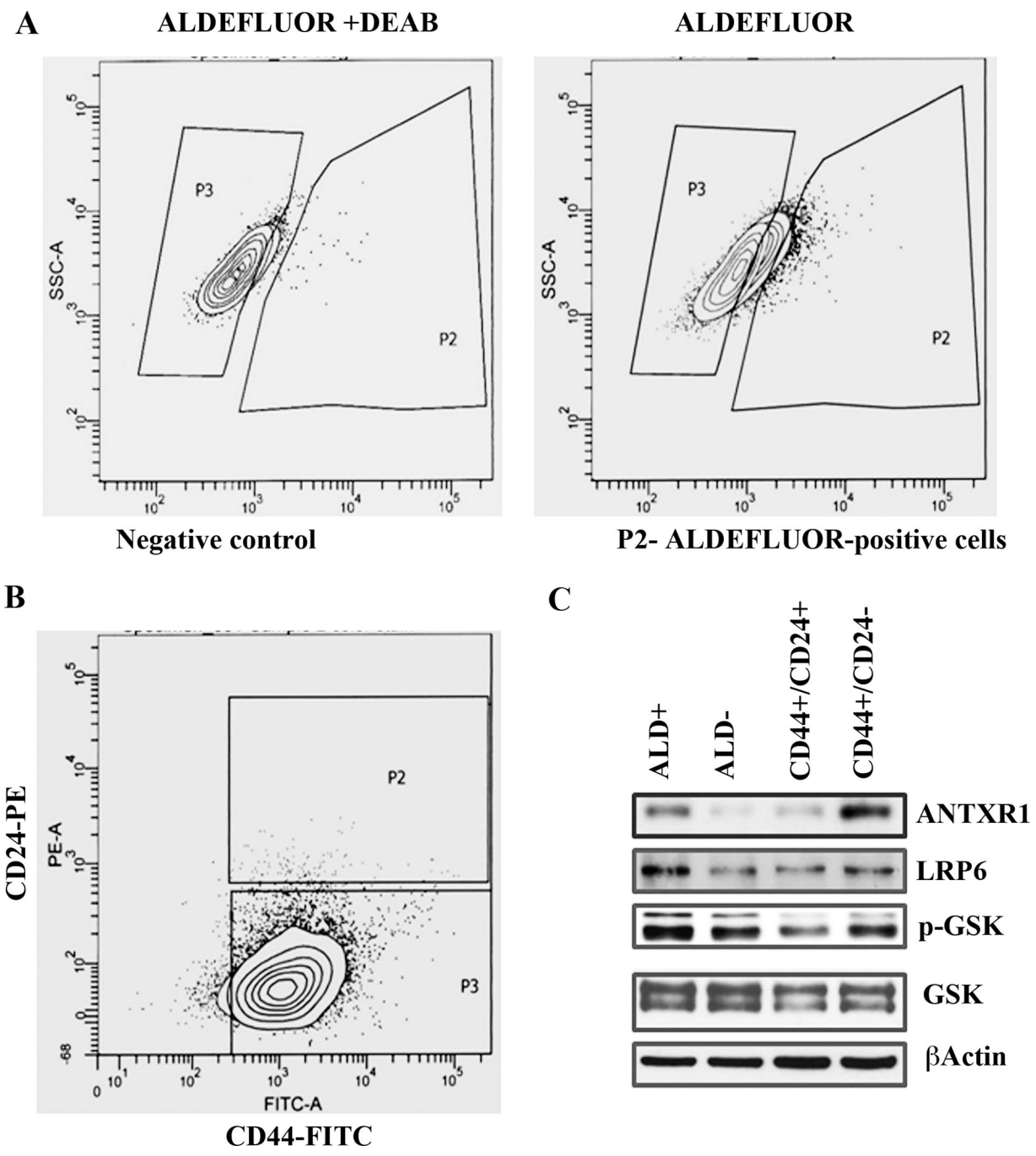

Fig. 4. ALDEFLUOR-positive and CD44+/CD24− CSCs from SUM149 cell line express higher levels of ANTXR1

A) ALDEFLUOR-positive cells in SUM149 cell line. ALDEFLUOR staining in the presence of DEAB served as a negative control and is shown on left. B) CD44 and CD24 staining pattern of SUM149 cells. C) ANTXR1 and Wnt pathway molecule levels in sorted ALDEFLUOR-positive, ALDEFLOUR-negative, CD44+/CD24−, and CD44+/CD24+ cells.

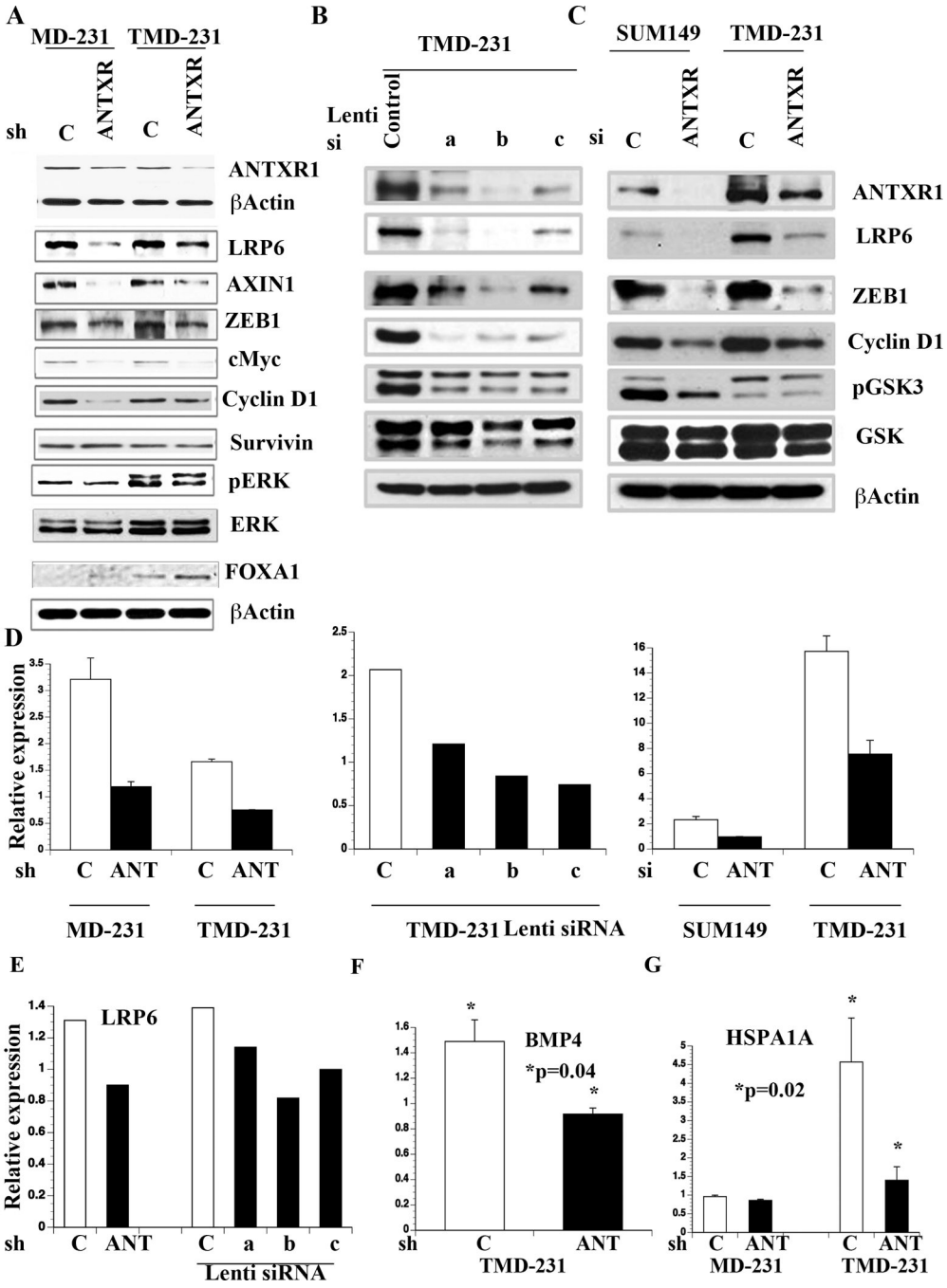

Fig. 5. The effects of ANTXR1 knockdown on Wnt pathway

A) Expression levels of various proteins downstream of Wnt pathway in control and ANTXR1 knockdown cells. B) Expression levels of various Wnt pathway molecules in TMD-231 cells infected with control or three independent ANTXR1 siRNA lentiviruses. C) Wnt pathway molecule expression in SUM149 and TMD-231 cells transiently transfected control luciferase or ANTXR1 siRNA. D) ANTXR1 mRNA levels in control and ANTXR1 sh/siRNA infected cells. E) LRP6 levels in control and ANTXR1 knockdown cells. F) BMP4 mRNA levels in control and ANTXR1 knockdown cells. G) HSPA1A expression in control and ANTXR1 knockdown cells (n>3).

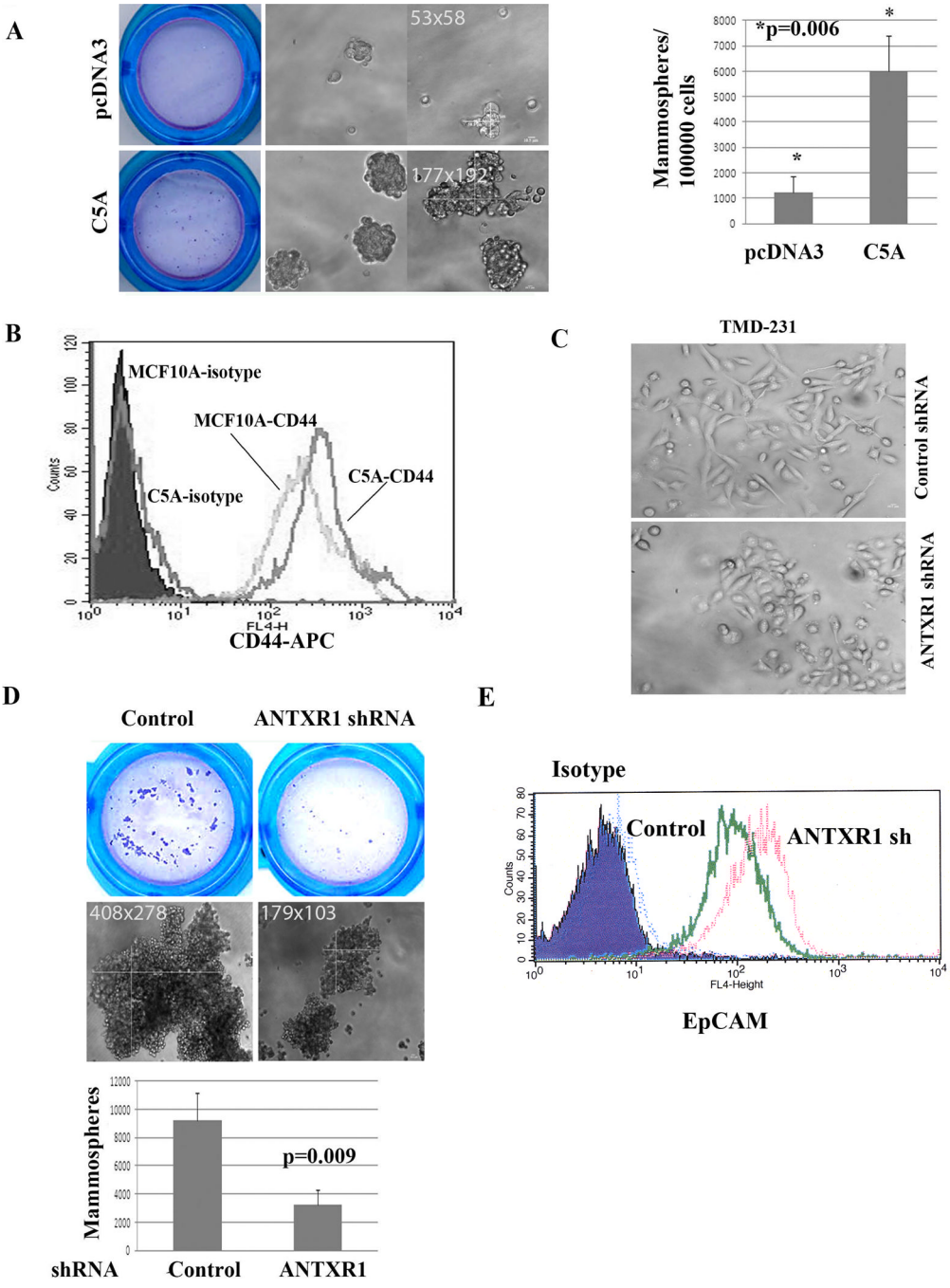

Fig. 6. ANTXR1 is essential for stemness phenotype

A) MCF-10A cells overexpressing C5A form larger and more mammospheres compared to parental cells. Mammospheres visualized upon Wright-Giemsa staining after filtering through a 40-micron filter along with photomicrographs from two fields are shown on left and numerical differences are shown in right. B) C5A overexpression leads to increased number of CD44+ MCF-10A cells. C) TMD-231 cells expressing ANTXR1 shRNA show epithelial morphology compared to parental cells, which are predominantly mesenchymal. D) TMD-231 cells expressing ANTXR1 shRNA display reduced mammosphere-forming capacity. Mammospheres visualized upon Wright-Giemsa staining (top), photomicrographs

(center) and numerical differences (bottom) are shown. E) ANTXR1 knockdown leads to increased cell surface levels of EpCAM.

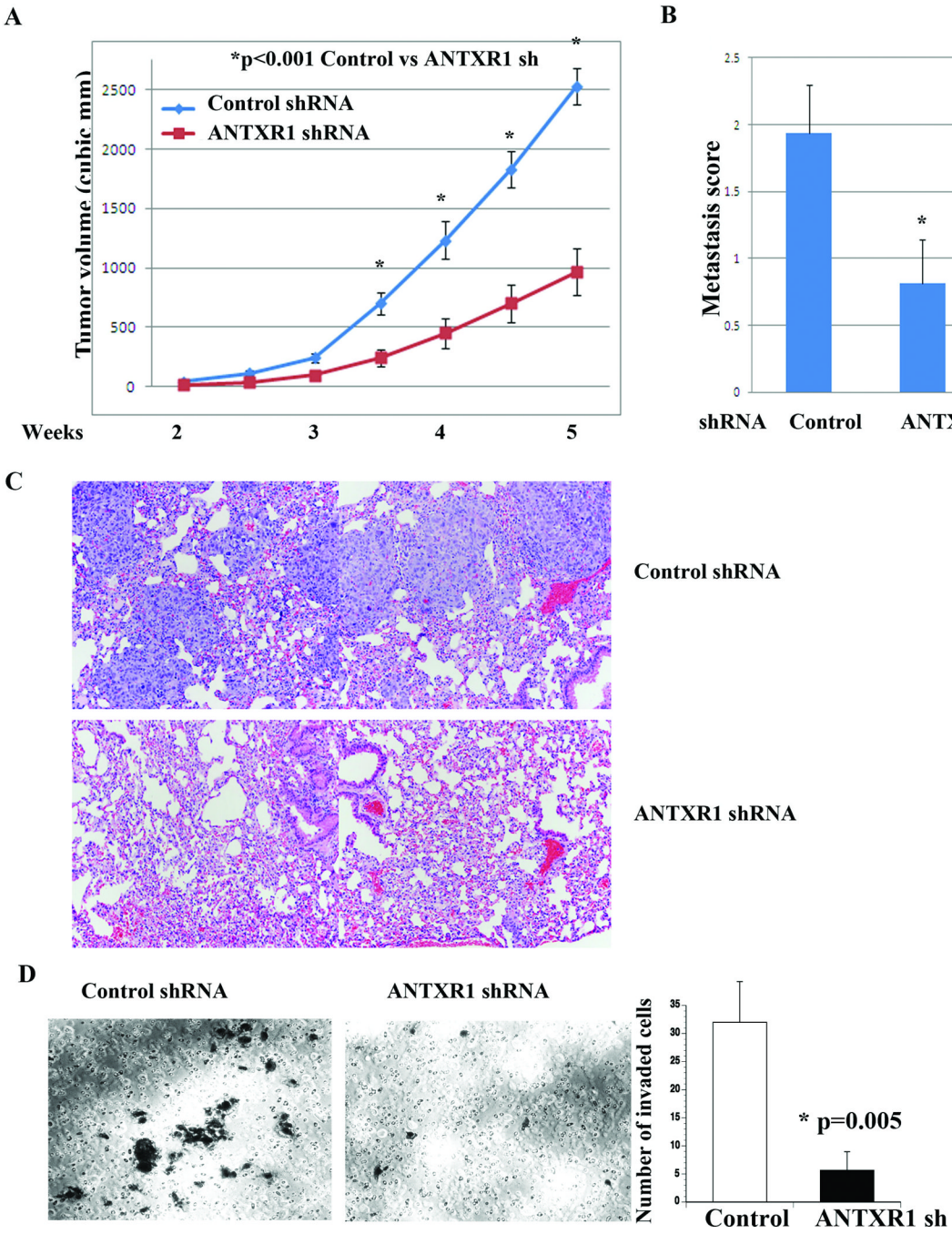

Fig. 7. ANTXR1 is essential for tumor growth and metastasis

A) Growth rate of mammary fat pad tumors in animals implanted with control or ANTXR1 shRNA expressing TMD-231 cells (n=8, average ± standard error). B) Lung metastasis index in animals with control shRNA or ANTXR1 shRNA expressing TMD-231 cells-derived mammary tumors. C) Representative H&E staining of lungs from control shRNA and ANTXR1 shRNA expressing TMD-231 cells. D) Matrigel invasion assay demonstrates reduced invasion of TMD-231 upon ANTXR1 knockdown. A representative field of invaded control and ANTXR1 knockdown cells is shown.